

Ohmic Contacts Formed on n-GaSb by Electrochemical Deposition

X. Li and A. G. Milnes

Department of Electrical and Computer Engineering, Carnegie Mellon University,
Pittsburgh, Pennsylvania 15213-3890, USA

ABSTRACT

Thin Ag, Au, Ni, and Pd films have been plated on n-GaSb by electrochemical deposition. The as-deposited structures have been examined by microscopy, surface profiling, and x-ray diffraction methods. Further examinations have been made after rapid thermal anneals to show the interactions of the metals with the GaSb and the development of ohmic contacts of low resistivities.

The formation of ohmic contacts on III-V semiconductors remains a problem of technological importance in spite of extensive studies already performed. The difficulty is to obtain reliable devices with low contact resistivities that do not degrade under operating conditions. This present work examines for GaSb the use of electrochemistry as a possible technique to obtain good ohmic contacts by electroplating of various metals. Electroplating is a simple, low-cost low-temperature process. There are also some drawbacks, the main one being the possible degradation, oxidation, or contamination of the semiconductor surface by the electrolyte. This may be responsible for the fact that electrodeposition of metals on semiconductors, except for silicon, has been very little employed in device fabrication.¹⁻⁴

GaSb has been drawing increasing attention because of its optoelectronic properties and high carrier mobility. GaSb has a direct bandgap of 0.72 eV at room temperature, and it forms interesting heterojunctions with various ternary and quaternary semiconductors. The optical properties of GaSb homojunctions have a particular potential for high-speed low-noise avalanche photodiode detectors (APDs).⁵

In this work, depositions of Ag, Au, Ni, and Pd onto n-GaSb are studied and interface compounds observed after heat-treatment. Electrical measurements are conducted for studying the ohmic contact behavior of such electroplated metal films to GaSb.

Experimental

Te-doped n-type ($1.9 \times 10^{17} \text{ cm}^{-3}$), (100) GaSb single-crystal wafers were used in this study. After trichloroethane, acetone, and methanol rinses, the GaSb wafer was etched by dilute HCl solution to remove the native oxide which may exist on the surface of the wafer. Then the wafer was immediately loaded into a sputtering system and 1500 Å of SiO₂ was deposited onto the GaSb by RF magnetron sputtering. After that a standard photolithography process with positive photoresist was used to define the areas where metals would be plated later. A buffered HF solution was used to open the rectangular pattern on the SiO₂ for transmission line measurements of contact resistivity, the dimensions being of the order $1800 \times 400 \mu\text{m}$. After the photoresist was removed, an indium back contact was made and heated to 250°C. The back side of the wafer was then protected by white wax to avoid metal deposition on that side of the wafer during plating of the pattern.

Electrolytic solutions were prepared with reagent-grade chemicals and deionized water. The Ag, Au, Ni, and Pd plating solutions contained AgCN (17 mM), KAu(CN)₂ (57 mM), NiCl₂ (0.23 M), and PdCl₂ (11 mM) as the source of the metal, respectively. The pH values of these solutions were adjusted to be between 10 and 11 by addition of NH₄OH, since we found alkaline solutions gave better results than more acidic solutions that are often studied for electrodepositions on GaAs. All depositions were per-

formed in a classical three-electrode electrochemical cell with a saturated calomel electrode (SCE) as the reference electrode. The anode was usually made of the metal to be plated (Ag, Au, Ni, and Pd). Various degrees of solution agitation were provided, the most effective being with the GaSb mounted on a rotating disk. The rotation speed was typically 120 rpm with the GaSb at a radius of about 1 cm. All plating solutions were at room temperature unless otherwise noted. The current-voltage curves and the current-time transients obtained were recorded on an X-Y-t recorder.

The thicknesses of the plated metals were monitored by a Tencor 2000 α -step surface profile measurement system. The structure and morphology of the metal films formed were studied by scanning electron microscopy (SEM). X-ray diffraction (XRD) with a copper source $\lambda(k, \text{Cu}) = 1.541 \text{ \AA}$ was used to identify and characterize intermetallic phases formed in the films. The thermal treatments of the plated GaSb were conducted in a Heatpluse 210 rapid thermal annealing system, AG associates, in a forming gas (90% N₂, 10% H₂) ambient. An HP 4145A semiconductor parameter analyzer was used to measure *I-V* curves of samples. A transmission line method (TLM)⁶ was applied to characterize the specific contact resistivity of the metal-GaSb contacts formed after heat-treatment. A four-probe measurement system was used to avoid the influence of probe contact resistance.

Some Principles of Electrochemical Deposition

Electrolytic deposition of metals is a complex process.⁷ Metal ions exist in solution as simple cations or as part of charged complexes. The deposition of metals is a function of mass transfer, the charge-transfer rate and its mechanism, nucleation, and crystal growth. In the case of a semiconductor electrode, there is the added complication of the space-charge layer inside the semiconductor which will influence the charge distribution of this electrochemical system. The first step for the deposition action is the process of nucleation and the nucleation behavior is a function of supersaturation (overpotential in electrolytic deposition) and interface energies.

A metal electrode immersed in a solution of an electrolyte develops a double layer at the metal-electrolyte interface.⁸ Electrons are always available in the surface of metal in large enough concentrations to interact with the metal ions in the solution, first for the formation of discharged atoms and then nucleation of the metal. Hence, for metal deposition on metal substrates only a small overpotential is required to overcome the nucleation energy barrier before deposition of the metal occurs.

In the case of a semiconductor electrode the situation is different, since a depletion region may occur in the semiconductor near the interface so that the Fermi level in the semiconductor becomes lined up with the redox energy of the electrolyte in the absence of applied voltage and associated current flow. For GaSb the electron affinity (conduction bandedge to vacuum level energy) has been determined by several methods.^{9,10} The values found are somewhat dependent on the sample preparation and on

* Electrochemical Society Active Member.

the measurement method. From a study of barriers in heterojunction structures such as InAs/GaAs, InAs/AlSb, and GaSb/AlSb, the valence band barriers ΔE_v are, respectively, 0.27, 0.10, and 0.45 eV. From these values it can be inferred that the electron affinity of GaSb is 4.0 ± 0.05 eV, which is close to the 4.07 eV value usually quoted for (100) GaAs.¹¹ Thus for n-GaSb doped 10^{17} cm⁻³ the Fermi level is about 4.02 eV below the vacuum level. We must now consider the redox levels of the plating solutions (at pH 11) used in these studies so that band diagrams can be presented.^{12,13} The solution of AgCN forms the redox couple



for which the standard reduction energy is -0.02 eV. For $\text{Ag}(\text{CN})_2$ the corresponding energy is -0.31 eV. For $\text{Au}(\text{CN})_2^-$ the energy is -0.595 eV and for $\text{Ni}^{2+} + 2e^- \rightarrow \text{Ni}$ the energy is -0.25 eV. The reactions for Pd compounds with the Pd^{2+} ion reduced to Pd have large positive energies such as +0.915 eV. The hydrogen couple $2\text{H}^+ + 2e^- \rightarrow \text{H}_2$ provides the reference zero. To relate these energies to the vacuum energy level, it is convenient to note that an SCE is at about -4.68 eV¹⁵ and is at 0.241 eV with respect to the zero of the H^+/H couple. Thus the H^+/H level is inferred to be at an energy of -4.44 eV. Hence the AgCN/Ag standard redox energy is -4.42 eV, and the $\text{Au}(\text{CN})_2^-/\text{Au}$ energy is at -3.845 eV with respect to the vacuum level.

Since the Fermi level of the n-GaSb is -4.02 eV with respect to the vacuum level, the standard redox energy for the AgCN/Ag couple is about 0.4 eV below the Fermi level and the $\text{Au}(\text{CN})_2^-/\text{Au}$ couple is about 0.175 eV above the Fermi level. If the pH of these solutions matches the pH 7 of water, the separated (not in contact) energy diagram would be as shown in Fig. 1a.¹⁴⁻¹⁶ For a solution that is higher in pH than a neutral pH of 7, there is a downward shift of the redox energy relative to the vacuum level and the semiconductor levels.¹⁵ Note that alternatively in some studies the SCE and redox levels are represented as fixed and the semiconductor bulk is considered to be charged so that its bandedges move up on the energy diagram. In a

form that may appear more usual to device people we consider the GaSb bulk to be grounded with respect to vacuum on the energy diagram and we allow the solution energy to move downward as the pH is increased.

This displacement of a pH change from 7 to 11 is $0.058 \times 4 = 0.232$ eV and is illustrated in Fig. 1b.¹ The redox potential of AgCN/Ag is then 0.632 eV below the GaSb Fermi level. Under contact conditions these potentials must align for a simple model (neglecting interface states in GaSb); hence electrons must come from the GaSb, and in contact there will be a positive depletion charge in the semiconductor and a bending up of the conduction and valance bands by 0.632 eV. Note that the uncertainty in the value of the electron affinity of GaSb will affect the precision of such numbers, but they are given as precise figures to allow the argument to be specific. We also made capacitance measurements to determine band bending, but these yielded no significantly different numbers.

The band bending that we have just discussed limits access of the silver solution to the electrons from the semiconductor and the semiconductor must be biased with an applied voltage to lower the depletion region and provide electrons if significant silver plating is to occur. Figure 1c shows the band bending that exists at a GaSb/electrolyte interface in the absence of applied voltage. With the AgCN solution (pH 11) in contact with Ag that has been deposited on the n-GaSb, the energy diagram in the absence of applied voltage lines up as shown in Fig. 1d. The Schottky barrier height is shown as 0.6 eV, and this tends to be true for many metals since, for GaSb, the height is controlled by interface states at 0.6 eV below the conduction band-edge. At the interface between the solution and the deposited silver, there is an abrupt dipole layer to bring the solution redox level in alignment with the Fermi level of the metal. For the redox numbers given in Fig. 1b, the flow of electrons from the semiconductor to the $\text{Au}(\text{CN})_2^-$ ions should not be impeded until Au is plated over the GaSb surface and the normal Schottky barrier Φ_B develops.

Possible tunneling effects and minority carrier effects at the semiconductor-solution interfaces have not been considered, in order to maintain a simple treatment.¹⁷

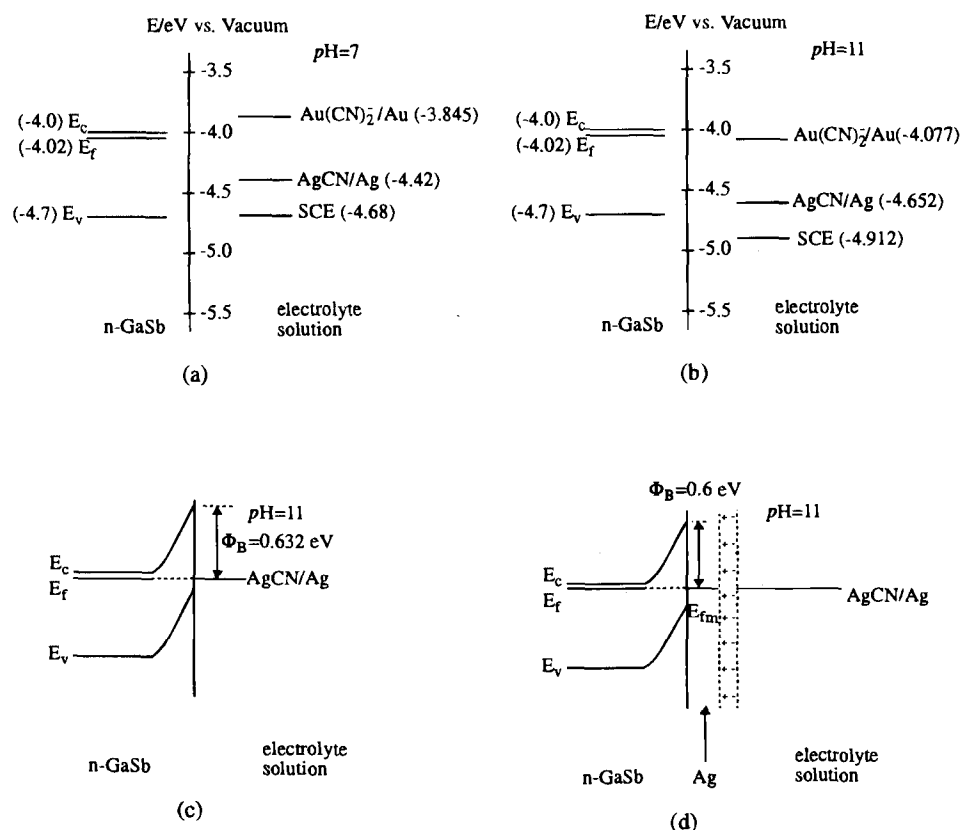


Fig. 1. GaSb and solution energy levels with respect to the vacuum level. (a) Levels in the absence of contact between the GaSb and solutions of pH 7; the dashed line is the Fermi level in the GaSb; (b) shift downward of the solution levels for a pH 11 relative to the GaSb; (c) energy band diagram of a n-GaSb/electrolyte contact at equilibrium without applied bias; (d) the n-GaSb/metal Schottky barrier energy diagram shown for zero applied voltage; the Φ_B barrier of 0.6 eV is determined by interface states about 0.1 eV above the valence bandedge.

Results and Discussions

Current-time transients and current-potential relation.—

In some plating studies it has not been unusual for a substantial overvoltage to be applied between the cathode and the anode for a short period of time to obtain initial nucleation that is favorable to the development of suitable metal grain size.¹²⁻¹⁴ However in this initial study of the plating of GaSb we elected to use a potentiostatic pulse method, namely, the GaSb was immediately dipped in the electrolyte after the cleaning process, and the electrode was held unbiased for almost zero time to limit possible oxidation of the surface before the application of the plating voltage. At $t = 0$, a dc voltage bias (height V_a , width t_d) was applied, and the transient in current $J(t)$ was recorded.

The current-time ($J-t$) transients at three different agitation conditions with an Ag anode and an AgCN solution (pH 11) at room temperature are shown in Fig. 2. $J-t$ transients which drop in time were presumably associated with metal ion diffusion limitations in the electrolyte.¹⁵ Mechanical agitation, with the sample on a disk rotating at 120 rpm, ensured a fresh electrolyte interface. The agitation condition also greatly affected the plating thickness of the metals. Figure 3 shows the profiles of plated Ag lines, masked by SiO₂, under three different agitation conditions: a, mechanical agitation; b, with ultrasonic agitation; and, c, no agitation; Edge enhanced plating is observed in the absence of the rotary agitation. This phenomenon is very similar to the edge enhanced etching discussed by Tan *et al.*¹⁸ This observation supports the view that the plating process is a diffusion-limited process. If no agitation, or even ultrasonic agitation is applied during the plating, the metal ion concentration above the GaSb plating window is reduced after the reductive reaction of metal ions takes place. Since no plating takes place above the SiO₂ mask area, the metal ion concentration outside the plating window is almost the same as the original one. Hence the metal ions will diffuse into the plating window through the electrolyte near the edge of the window. This causes the metal ion concentration near the edge to be higher than that of the middle portion of the pattern. As a consequence of this concentration gradient, the metal plated without proper agitation will display a nonuniform surface profile. All subsequent results were for conditions of rotary agitation.

As shown in Fig. 2, the $J-t$ transient of silver plating with rotary agitation reached a near-constant value within a few tens of seconds after an initial peak. The plating current for gold plating (not shown) declined steadily in the time span examined, if the voltage between cathode and anode was kept constant. The plating currents in Ni and Pd plating rose with the plating time.

The factors that determine the shape of the $J-t$ transients have been discussed by Bindra *et al.*,² Allongue *et al.*,¹⁴ and

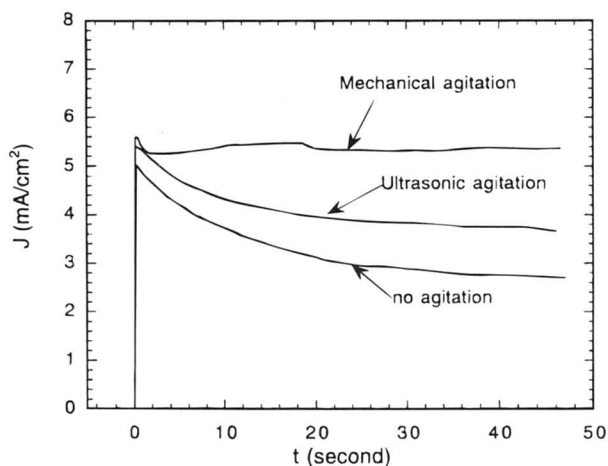


Fig. 2. Current-time transients for silver deposition on n-GaSb at different agitation conditions with a Ag anode.

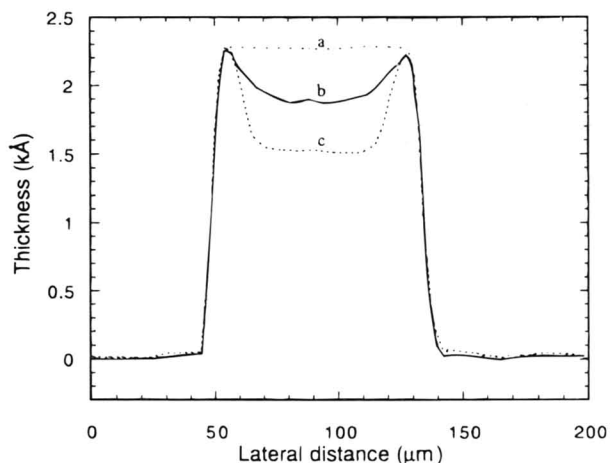


Fig. 3. Surface profile of Ag plated GaSb under different agitation conditions: a, rotary agitation; b, ultrasonic agitation; c, no agitation. The exposed region was a strip about 100 μm wide and masked by SiO₂ on each side that was subsequently removed.

Oskam *et al.*,¹⁵ for Ag, Pb, and Pd plated on semiconductors such as GaAs, GaP, CdS, ZnO, and SnO₂. The rising part of the current transient suggests nucleation with three-dimensional growth of the nuclei and falling current suggests the onset of diffusion control. Another factor in the shape of the $J-t$ transient may be associated with the area *vs.* time transient from initially a simple semiconductor/solution barrier to one in parallel with a growing semiconductor/metal/solution structure. Hence interpretation of the shape of the $J-t$ transients is not always easy. The illustration in Fig. 4a represents the plating bath and defines the voltages V_a and V , and shows the grounding of the GaSb to set the vacuum level as the reference energy.

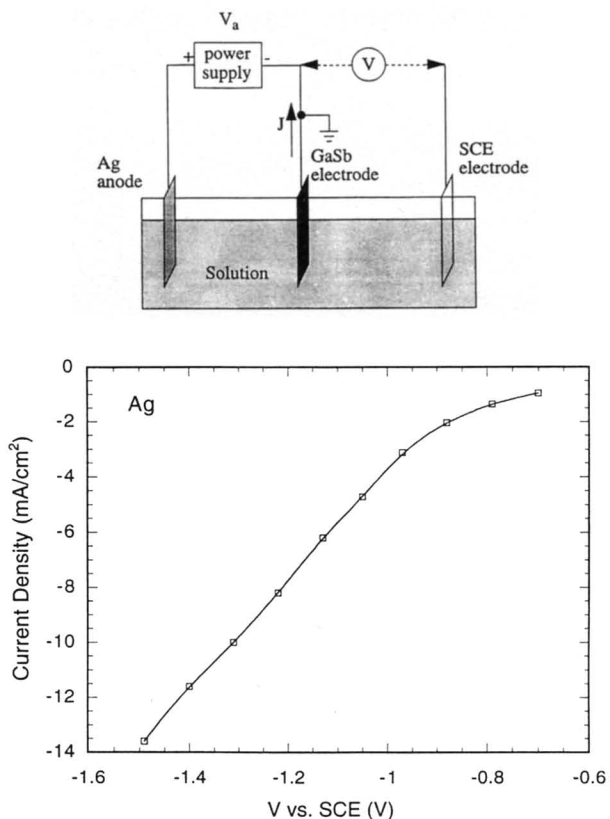


Fig. 4. Silver plating cell scheme (a, top) to define the voltages V_a and V , and (b, bottom) current density vs. voltage of the GaSb electrode with respect to the SCE reference electrode.

In plating studies the current density J is often plotted against the substrate to solution potential as measured by a high-impedance voltmeter with respect to an SCE electrode. For the Ag plating solution and a Ag anode the result in Fig. 4b is seen to suggest a Schottky barrier-type curve with a series resistance. For an Au plating solution and a Au anode, the curve (not shown) shows a Schottky barrier-type form with less series resistance effect. For Ni and Pd plating, the results (Fig. 5) are even more like regular Schottky barrier I - V curves. For comparison we show a Ni/n-GaSb (dry) diode characteristics obtained after sputtering the Ni on the n-GaSb. This diode curve has been displaced along the voltage axis by -0.89 V to allow for the potential of the Ni plating solution, by considering SCE and vacuum levels, and the match is seen to be reasonably satisfactory in view of the various uncertainties in the numbers, mentioned earlier, and the role of interface states.

Morphology studies.—The parameters which determine deposition include: (i) the electrolyte composition (the ion chemistry, the concentration, the pH, etc.); (ii) the conditions of the cathode surface initially and during the deposition; (iii) the applied bias voltage (which controls the current density) and whether steady-state or pulsed voltage conditions are applied, and (iv) the changes of these factors during the time of deposition.^{19,21} Nucleation is a complex phenomenon, but as a general trend, for a given solution the current density controls the density of nuclei and therefore influences the morphology of the deposited metal: the greater the current density the larger the density of nuclei.

In order to study how such factors influenced the properties of metal plating on a GaSb electrode, different plating current densities were used to plate about 2500 Å of silver on n-GaSb. The plating times required for the chosen thickness were longer at low current density than would be expected for a rate directly proportional to current, suggesting slow initial nucleation. We did not repeat the kind of study of initial nucleation processes performed by Allongue and Souteyrand¹⁴ for Pt electroplating on n-GaAs. The current density vs. applied voltage is shown in Fig. 6 for an Ag anode (as in Fig. 4) and for a Pt anode for comparison. The 1 V shift of the Pt anode curves at close to zero current about matches the difference between the work functions of Pt (5.65 eV) and Ag (4.64 eV). However when current is flowing and plating is taking place, the spacing between the two curves becomes greater, presumably because solution processes such as Ag dissolution at the Ag anode and actions at the Pt anode begin to become important and add potentials.

The surface morphologies of plated Ag films were studied by scanning electron microscopy (SEM). As shown in

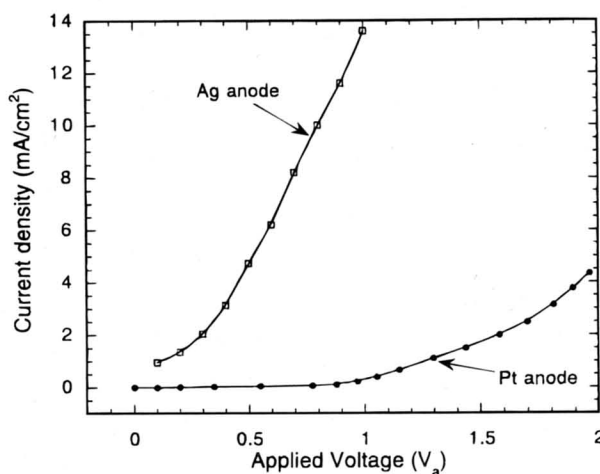


Fig. 6. Current density vs. anode to cathode voltage applied with Ag or Pt anodes for the AgCN solution.

Fig. 7, the density of grains for Ag plated at a current density of 1.5 mA/cm² was about $4 \cdot 10^9$ cm⁻², and the average grain size was about 2000 Å. When the plating voltage and current density were increased, the average grain size decreased. At a plating current density of 3.5 mA/cm², the density was about $2 \cdot 10^{10}$ cm⁻² and the average Ag grain size was about 500 Å. Compared to the TEM results reported by Allongue and Souteyrand¹⁴ for Pt plating on GaAs, the density of our observed nuclei is one or two orders of magnitude lower. The low density might be related to the coalescing of initial nuclei into small clusters or related to the actions at the semiconductor-metal interface, but this has not been investigated. Deposition of metals on all substrates begins with nucleation of minute clusters of the new phase formed at energetically favorable sites on the sub-

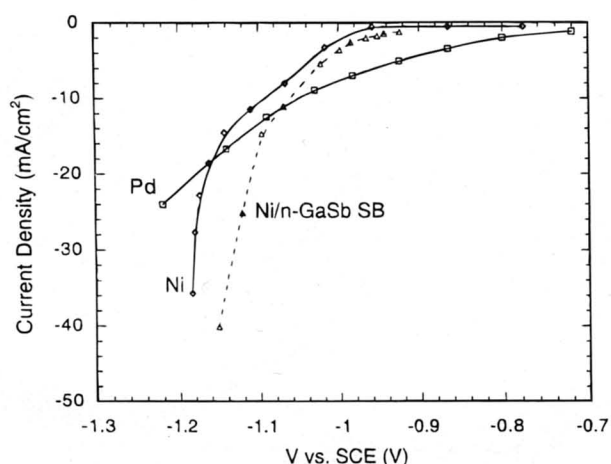


Fig. 5. Current density vs. the voltage of the GaSb electrode with respect to the SCE electrode for Ni and Pd electroplating cells. The dashed line is the J vs. V characteristic for a (dry) sputtered Ni/n-GaSb Schottky barrier, displaced by 0.89 V.

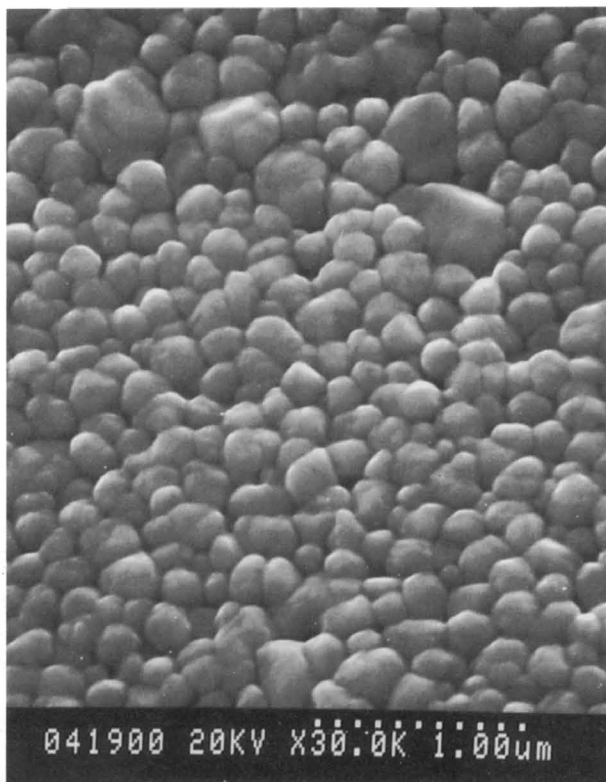


Fig. 7. SEM picture of a Ag film (~ 2500 Å) plated on n-GaSb. The plating current density was 1.5 mA/cm² and the time 8 min.

strate. In the case of semiconductor electrodes, even small clusters consisting of only a few metal atoms in the contact with semiconductor constitute localized Schottky barriers.¹ These contacts are in parallel with the semiconductor-electrolyte contact and thus modify the space-charge layer. For a metal with a relatively low work function (like Ag) the Fermi level of the metal lies between the semiconductor Fermi level and that of the electrolyte. If the barrier at the metal-semiconductor interface is lower than the original barrier between the semiconductor and the electrolyte before metal is deposited, the depletion layer width at the metal-semiconductor contact decreases, and the surface electron concentration increases. Then the metal nuclei become preferential sites for deposition and there is less further nucleation on the substrate. Such a system therefore influences grain size.

For the plating of a metal with higher work function (like Pd), the Fermi level of the metal is well below both the semiconductor Fermi level and that of the electrolyte. If the initial minute metal clusters form a high barrier between the semiconductor and the metal, they make the surface electron concentration decrease at the semiconductor-metal interface. Thus charge-transfer on the top of existing metal nuclei is then more restricted by the availability of electrons so that a metal ion (or metal ion complex) is approaching the electrode surface would find it more favorable to react on the exposed parts of the semiconductor surface. This process would encourage progressive nucleation and therefore a larger density of nuclei may be expected.

For Au plating, as for Ag, the density of nuclei increased and the grain size decreased for the current density range studied (1.5 to 7 mA/cm²). The shapes of the Au grains were irregular, as seen in Fig. 8 for deposition at 4 mA/cm², and the surface coverage of the gold film was poor. Further investigation of the gold plating process would be desirable since there are many parameters that might be varied.^{19,20} For GaSb the formation of [Au, Sb] compounds is possible, whereas there are no [Au, As] compounds for Au reacting with GaAs.

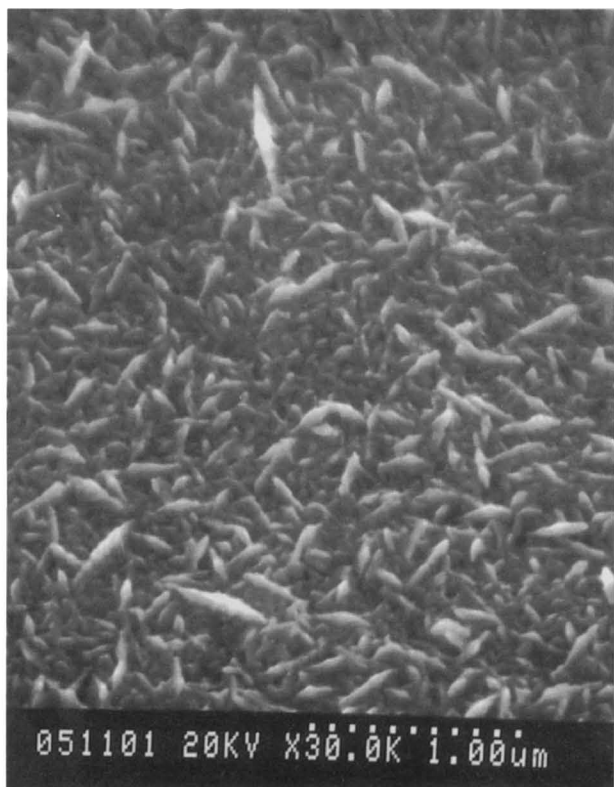


Fig. 8. SEM picture of a Au film ($\sim 2500 \text{ \AA}$) plated on n-GaSb. The plating current density was 4 mA/cm² and the time 3 min.

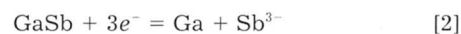
The grain size of Ni plated at a low current density of 1.5 mA/cm² was large (5000 Å), but with the increase of the plating current to 8 mA/cm², the grain size decreased two orders of magnitude to about 50 Å. The surface coverage by the Ni film was comparable to that for the Ag film and was much better than for the gold film (which tended to be porous).

The Pd films plated on n-GaSb were perhaps influenced in initial nucleation by the tendency of Pd to be autocatalytic on many surfaces. The current density range 2 to 12 mA/cm² was examined, and it was found that, compared with Ag, Au, and Ni films, the surface texture and nuclei density did not change much with change of the plating current density.

Ohmic contact studies.—The contact behavior of metal-plated n-GaSb was studied by the transmission line method (TLM).⁶ The *I-V* characteristics of a Ag/n-GaSb contact are shown in Fig. 9. The as-plated contact shows a nonlinear (rectifying) *I-V* characteristic due to the Schottky barrier between the Ag and n-GaSb. After rapid thermal annealing (RTA) in forming gas at 400°C for 10 s, the contact becomes quite ohmic.

To study the effect of the plating conditions on the performance of the ohmic contact, Ag samples were prepared at different plating current densities as described in the previous section. After the 450°C RTA and ohmic contact measurement, the specific ohmic contact resistivity (ρ_c) was obtained as a function of plating current density. From Fig. 10, one can see that the sample prepared by the lowest current density produced the lowest contact resistivity. The samples prepared for a current density range from 3.5 to 13 mA/cm² all had similar contact resistivities.

For a large plating voltage the conduction band of n-GaSb may move relative to the cathodic dissolution potential E_{DC} and be sufficiently close that a reductive decomposition of the n-GaSb surface may occur according to a reaction similar to that reported for n-GaAs,²¹ namely



The E_{DC} is not known for GaSb, since very little research has been done on the electrochemical properties of GaSb. However, the E_{DC} for GaAs is -0.5 V/SCE at pH 11. Based on the above considerations, the samples that are prepared at a high plating voltage may have an inhomogeneous interface between the GaSb and the Ag, and this probably leads to the higher contact resistivities shown in Fig. 10.

To get some idea of the optimal RTA conditions, annealing temperatures of 400, 450, and 500°C were applied to the Ag plated samples. The ohmic contact resistivity variation with annealing temperature in this range was not large. However as stated before, the sample prepared at a low current density (1.5 mA/cm²) presented a lower con-

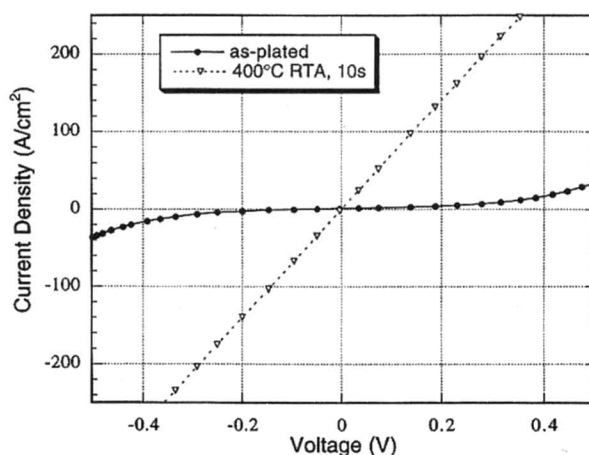


Fig. 9. *J-V* characteristics of Ag/n-GaSb contacts prepared by plating. Linearity is produced by 400°C rapid thermal annealing.

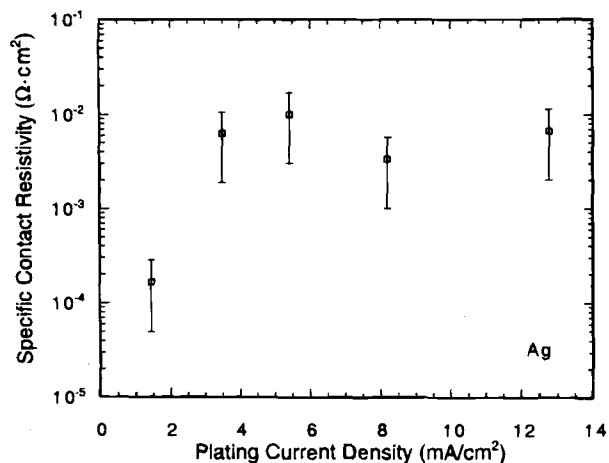


Fig. 10. The specific contact resistivities after RTA at 400°C of Ag/n-GaSb samples prepared at various plating current densities.

tact resistivity. The 450°C RTA sample showed the lowest contact resistivity ($\sim 2 \cdot 10^{-4} \Omega \cdot \text{cm}^2$). Compared to the results²² for Ag ohmic contacts in p-type GaSb with similar doping (10^{17}cm^{-3}), the ρ_c of the contacts on n-GaSb was one order of magnitude lower. For 400 and 450°C RTA, there was no significant change in surface morphology; however for the anneal at 500°C the Ag film lost its shining finish. This observation indicates that there was extensive reaction at the GaSb-Ag interface. X-ray diffraction (XRD) was used to identify the phases formed in our samples. The XRD results of an as-plated sample showed only the GaSb substrate peak and silver peaks, indicating no interface reaction as-plated. After a 400°C RTA, several peaks corresponding to various Ag-Ga and Ag-Sb alloys emerge as shown in Fig. 11, and this must relate to the ohmic contact behavior after annealing. After a 500°C RTA, peaks corresponding to Ag can no longer be detected. This indicates that the reaction between the Ag and the GaSb was very extensive.

For the Au/n-GaSb contact, the as-plated sample was also rectifying. After a 400°C RTA, the contacts became ohmic, the specific ohmic contact resistivity (ρ_c) was about $1 \cdot 10^{-4} \Omega \cdot \text{cm}^2$ for a plating current density of 4 mA/cm² and $2 \cdot 10^{-2} \Omega \cdot \text{cm}^2$ for 7 mA/cm². The results are similar to those for Ag, since high plating current density produced high contact resistance. The ρ_c was measured for various annealing temperatures for Au/n-GaSb samples prepared at the two different current densities. The results

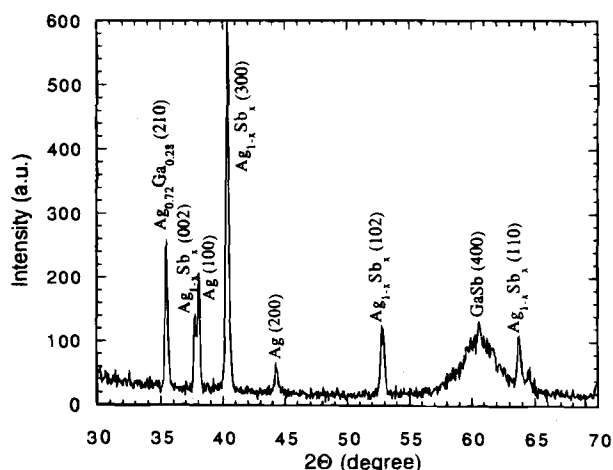


Fig. 11. X-ray diffraction results for a 400°C, 10 s annealed Ag/n-GaSb sample.

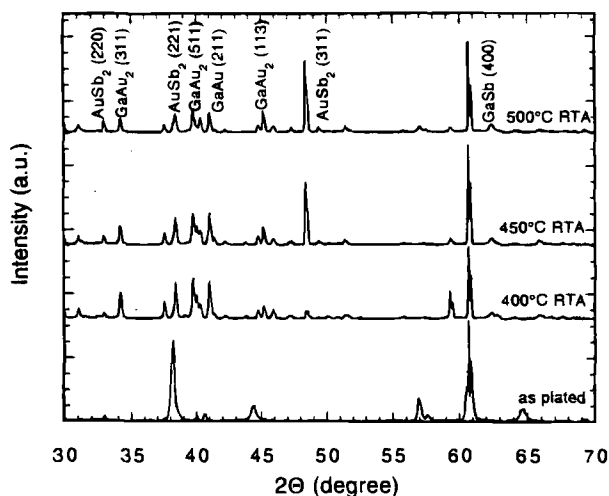


Fig. 12. XRD results for Au/n-GaSb samples after RTA (10 s) at various temperatures.

showed that 400°C RTA was an appropriate temperature to obtain ohmic contacts for Au/GaSb. The XRD results for Au/GaSb samples are shown in Fig. 12. It should be noticed that the as-plated sample already showed some Ga-Au and Sb-Au compounds. Obviously there is a considerable reaction between GaSb and Au during the $\text{KAu}(\text{CN})_2$ (pH 11) room temperature plating process. This was probably a factor in the irregular grain shapes shown in Fig. 8.

The Ni/n-GaSb contact was unusual among the four metals studied in this work. The Ni/n-GaSb contact remained rectifying even after a 600°C RTA. The XRD pattern (Fig. 13) did not change much with the annealing, the 600°C RTA sample was almost the same for the as-plated sample. Possibly a very stable insulating layer such as an oxide might have been formed during the plating process, but we did not detect such a layer in the XRD study.

For the Pd/n-GaSb contact, in agreement with the SEM study of grain size, the plating current had little effect on the value of ρ_c . The as-plated Pd/n-GaSb contact was rectifying, and after a 450°C RTA the contact became ohmic. This matches the results obtained from samples prepared by thermal evaporation of Pd onto GaSb.²³ The specific contact resistivities plotted as a function of annealing temperature are shown in Fig. 14. The value of ρ_c is seen to be higher than for Ag and Au contacts to n-GaSb. The

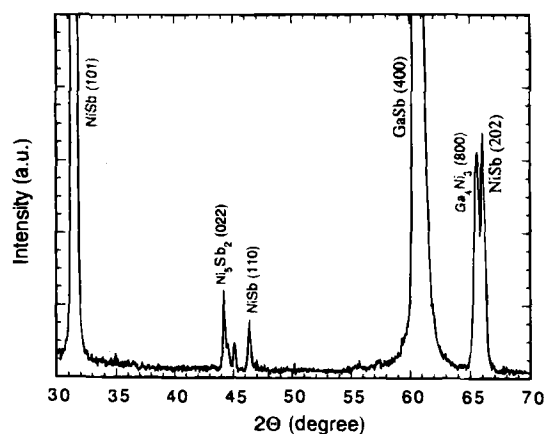


Fig. 13. XRD results for an as-plated Ni/n-GaSb sample, showing that substantial interaction of the Ni with GaSb has occurred even with the room temperature plating.

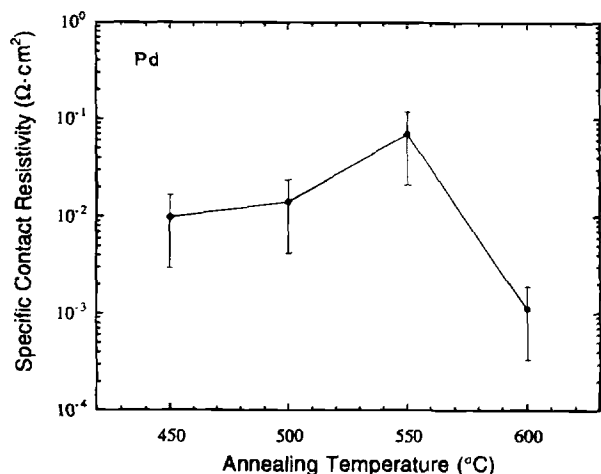


Fig. 14. Ohmic contact resistivities vs. annealing temperatures for Pd/n-GaSb samples.

XRD results of Pd/GaSb samples after various thermal treatments are shown in Fig. 15.

Electroless plating on GaSb.—Electroless plating of Pd onto GaSb was also attempted. Various solutions with various pH values (pH 1 to 12) and different Pd²⁺ ion concentrations were used to plate Pd onto GaSb at temperatures in the range from 35 to 80°C. Undercutting of the SiO₂ mask on the GaSb substrate by the plating solution tended to occur. Possibly the reason for this is that the energy required for the exchange reaction between Pd²⁺ and GaSb is comparable to or smaller than the energy required to reduce Pd²⁺ to Pd. This undercutting behavior is related to the chemical properties of GaSb, and was not reported for Pd electroless plating on GaAs.²⁴⁻²⁶

Conclusions

Electroplating of n-GaSb from Ag, Au, Ni, and Pd solutions has been examined. Such films, of thickness about 2500 Å, have been shown to result in ohmic contacts of specific resistivities in the range of 5 × 10⁻³ to 5 × 10⁻⁴ Ω·cm² if given rapid thermal annealings for 10 s at 400 or 450°C.

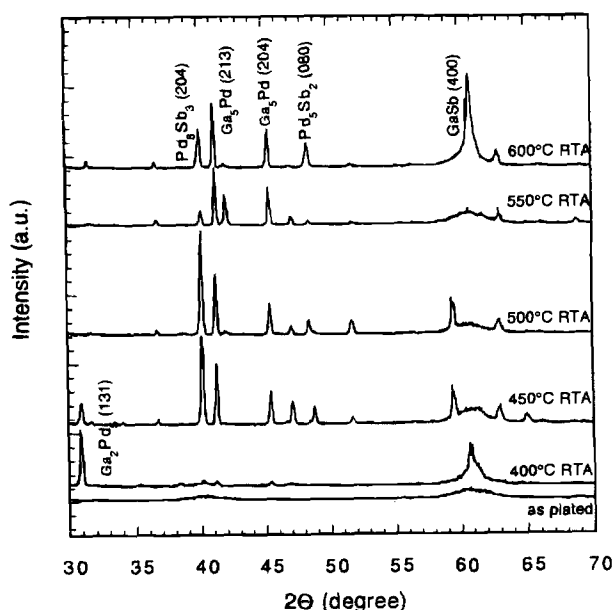


Fig. 15. XRD results for Pd/n-GaSb samples, showing the effects of thermal annealing at 450 to 600°C peak temperatures.

XRD studies show the formation of gallium-metal and metal-antimony compounds after RTA treatments. High plating rates tended to give decreased grain size with less porosity but higher contact resistances. The Au films plated from KAu(CN)₂ solution (pH 11) were less satisfactory than the Ag or Ni films because of the unusual grain structure probably associated with attack on the GaSb surface. Solutions that are used for plating of Si and GaAs were found not to be specially satisfactory for electroplating of GaSb. Further studies are needed before electroplated films on GaSb may be evaluated against sputtered or vacuum-evaporated films.

Acknowledgments

This study was supported in part by NSF Grant No. DMR 91 21048. Helpful assistance was given by Professor A. Z. Li and Professor S. S. Tan.

Manuscript submitted July 24, 1995; revised manuscript received about Nov. 12, 1995.

Carnegie Mellon University assisted in meeting the publication costs of this article.

REFERENCES

1. P. Allongue and E. Souteyrand, *J. Vac. Sci. Technol.*, **B5**, 1644 (1987).
2. P. Bindra, H. Gerischer, and D. M. Kolb, *This Journal*, **124**, 1012 (1977).
3. M. Ludwig, G. Heymann, and P. Janietz, *J. Vac. Sci. Technol.*, **B4**, 485 (1986).
4. J. T. Lue, *Appl. Phys. Lett.*, **34**, 688 (1979).
5. A. G. Milnes and A. Y. Polyakov, *Solid State Electron.*, **36**, 803 (1993).
6. H. H. Berger, *ibid.*, **15**, 145 (1972).
7. J. A. Harrison and H. R. Thirsk, in *Electroanalytical Chemistry*, Vol. 5, A. J. Bard, Editor, p. 67, Marcel Dekker, Inc., New York (1971).
8. W. Blum and G. B. Hogaboom, *Principles of Electroplating and Electroforming*, p. 45, McGraw-Hill, New York (1949).
9. M. Yano, K. Yoh, Iwawaki, Y. Iwai, and M. Inou, *J. Crystal Growth*, **111**, 397 (1991).
10. S. P. Kowalczyk, W. J. Shaffer, E. A. Kraut, and R. W. Grant, *J. Vac. Sci. Technol.*, **20**, 705 (1982).
11. A. G. Milnes and D. L. Feucht, *Heterojunctions and Metal-Semiconductor Junctions*, p. 8, Academic Press Inc., New York (1972).
12. A. J. Bard, R. Parsons, and J. Jordan, Editors, *Standard Potentials in Aqueous Solution*, p. 316, Marcel Dekker Inc., New York (1985).
13. A. J. Bard, A. B. Bocarsly, F. R. F. Fan, E. G. Walton, and M. S. Wrighton, *J. Chem. Soc.*, **102**, 3671 (1980).
14. P. Allongue and E. Souteyrand, *J. Electroanal. Chem.*, **286**, 217 (1990); P. Allongue and E. Souteyrand, *ibid.*, **362**, 79 (1993); P. Allongue, E. Souteyrand, and L. Allenmand, *ibid.*, **362**, 89 (1993).
15. G. Oskam, D. Vanmaekelbergh, and J. J. Kelly, *Electrochim. Acta.*, **38**, 291 (1993).
16. G. Horowitz, P. Allongue, and H. Cachet, *This Journal*, **131**, 2563 (1984).
17. S. R. Morrison, *Electrochemistry at Semiconductor and Oxidized Metal Electrodes*, Chap. 5, Plenum Press, New York (1980).
18. S.-S. Tan, M. Ye, and A. G. Milnes, *Solid State Electron.*, **38**, 17 (1995).
19. *The Properties of Electrodeposited Metals and Alloys*, 2nd ed., W. H. Safranek, p. 165, American Electroplaters and Surface Finishers Society, Orlando, FL (1986).
20. J. W. M. Jacobs and J. M. G. Rikken, *This Journal*, **136**, 3633 (1989).
21. S.-M. Park and M. E. Barber, *J. Electroanal. Chem.*, **99**, 67 (1979).
22. A. G. Milnes, M. Ye, and M. Stam, *Solid State Electron.*, **37**, 37 (1994).
23. Y. K. Su, N. Y. Li, and F. S. Juang, *ibid.*, **34**, 426 (1991).
24. D. Lamouche, J. R. Martin, P. Clechét, G. Haroutiounian, and J. P. Sandino, *This Journal*, **131**, 2563 (1984).
25. D. Lamouche, P. Clechét, J. R. Martin, G. Haroutiounian, and J. P. Sandino, *ibid.*, **134**, 692 (1987).
26. G. Stremsoerfer, H. Perrot, J. R. Martin, and P. Clechét, *ibid.*, **135**, 2882 (1988).